2015 15th International Conference on Control, Automation and Systems (ICCAS 2015)
Oct. 13-16, 2015 in BEXCO, Busan, Korea

Kinect Camera Sensor-based Object Tracking and Following of Four wheel Independent Steering Automatic Guided Vehicle Using Kalman Filter

Amruta V. Gulalkari[1], Dongbo Sheng[1], Pandu Sandi Pratama[1], Hak Kyeong Kim[1], Gi Sig Byun[2] and Sang Bong Kim[1*]

[1] Department of Mechanical and Automotive Engineering, Pukyong National University, Busan, 608-739, Korea (kimsb@pknu.ac.kr) * Corresponding author

[2] Department of Control and Instrumentation Engineering, Pukyong National University, Busan, 608-739, Korea (gsbyun@pknu.ac.kr)

Abstract: This paper presents a Kinect camera sensor-based object tracking and following system for the four wheel independent steering automatic guided vehicle (4WIS-AGV) using Kalman filter and backstepping control method. To accomplish this task, the following steps are executed: Firstly, a blue colored object is detected by the Kinect camera sensor using a color-based object detection method and its center coordinates inside the RGB image frames are obtained. The global position coordinates of the detected object and the 4WIS-AGV are obtained using Kinect depth data and NAV200 navigation system. Secondly, a Kalman filter is used to estimate the global position and velocity coordinates of the detected moving object. Thirdly, a backstepping control method using Lyapunov function is adopted for the 4WIS-AGV to perform the object following task. Finally, simulation and experiment are performed to verify the effectiveness of the proposed system. The results show that the 4WIS-AGV with Kinect camera sensor can follow the moving object well with the designed controller.

Keywords: 4WIS-AGV, Kinect camera sensor, Kalman filter, Backstepping control, Lyapunov function, Object following.

1. INTRODUCTION

Developing object detection, tracking and following systems is one of the interesting topics of research in the field of autonomous robotics. Mobile robot equipped with camera sensor can analyze its environment to perform object detection and tracking well. There are several researches for object tracking and following using various mobile robotic platforms [1, 2]. In [3, 4], cameras were installed on simple differential wheeled configuration. The problems with such wheeled configuration are its limited maneuverability and flexibility. The selection of camera is also an important issue. Moreover, depth data is the basic requirement in the such systems. In [5], conventional cameras are utilized for performing the above mentioned tasks using stereo vision technique. However, image processing using stereo vision is quite inconvenient process as it has correspondence matching issues and thus depth calculation becomes a complex process. Tracking of the moving object is also an important problem considered in such systems. Furthermore, the crucial part is to choose the appropriate control law that helps the system to achieve better stability. In [6], controller was designed using Fuzzy logic control method. However, in fuzzy logic-based controller, selection of membership function is not an easy task. Membership function must be carefully chosen to achieve maximum performance and selection requires much effort.

To deal with these problems, this paper proposes a Kinect camera sensor-based object tracking and following system for the four wheel independent steering automatic guided vehicle (4WIS-AGV) based on Kalman filter and backstepping control method. The four wheel independent steering configuration of the AGV exhibits high maneuverability and more flexibility since each wheel orientation is adjusted separately. Because of this reason, 4WIS-AGV can move in any desired direction. To overcome the camera problem, a low-cost RGB-D Kinect camera is chosen for this system to be is able to provide the direct depth information. Among several tracking algorithms [7, 8] and controller methods, Kalman filter algorithm and backstepping control method are adopted for the proposed system to track and follow the moving object, respectively. With the backstepping control method, system stability is assured for the 4WIS-AGV.

This paper presents a Kinect camera sensor-based object tracking and following system for the four wheel independent steering automatic guided vehicle (4WIS-AGV) using Kalman filter and backstepping controller. To do this task, the followings are executed. Firstly, a candidate blue colored object is detected by the Kinect camera sensor using a color-based object detection method and its center coordinates inside the RGB image frames are obtained. The global position coordinates of the detected object and the 4WIS-AGV are obtained using Kinect depth data and NAV 200 navigation system. Secondly, the Kalman filter is used to estimate the global position and velocity coordinates of the detected moving object. Thirdly, a backstepping control method using Lyapunov stability theory is adopted for the 4WIS-AGV to perform the object following task. Finally, simulation and experiment are performed to verify the effectiveness of the proposed system. The results show that the 4WIS-AGV with Kinect camera sensor can follow the moving object well with the designed controller.

978-89-93215-09-0/15/$31.00 ⓒICROS

2. SYSTEM DESIGN

Fig. 1 shows the Kinect camera sensor-based object tracking and following 4WIS-AGV system used in this paper.

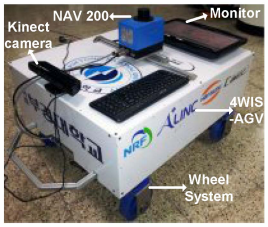

Fig. 1 4WIS-AGV system.

The 4WIS-AGV configuration uses four wheel systems. Each wheel system has two high power DC motors; one is for driving and another is for steering. This 4WIS-AGV is controlled by Industrial PC and eight ATmega128 microcontrollers (one for each motor). Each motor has a separate motor driver and is controlled independently by the Atmega128 microcontroller.

The sensors used for this system consist of a Kinect camera sensor, a laser navigation system (NAV-200) and eight encoders. The Kinect camera sensor is mounted on the front side of the 4WIS-AGV to capture both RGB and depth images at the speed of 30 frames/sec. For this system, the Kinect camera uses default mode of operation that has the operating range of 0.8 m to 4 m. The NAV-200 is attached on the top center of the 4WIS-AGV and is used as a positioning sensor and eight encoders are used to measure wheel steering angles of the steering motors and angular velocities of the driving motors. A monitor is placed on the back side of the 4WIS-AGV and is used as an input device for the 4WIS-AGV system.

3. KINEMATIC MODELING

The configuration of 4WIS-AGV system for kinematic modeling is shown in Fig. 2.

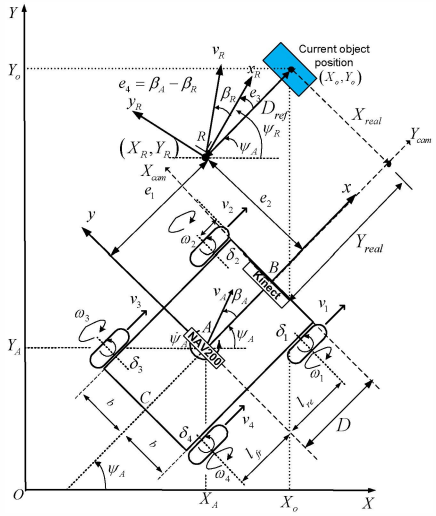

Fig. 2 Configuration of the 4WIS-AGV system.

where

OXY : Global coordinate frame

Axy : Local coordinate frame

$Rx_R y_R$: Reference coordinate frame

$BX_{cam}Y_{cam}$: Kinect coordinate frame

X_A, Y_A : Current positions of the 4WIS-AGV (m)

v_A : Vehicle linear velocity (m/s)

ω_i, δ_i : i^{th} wheel angular velocity (rpm) and the i^{th} wheel steering angle (rad), respectively, for $i = 1,...,4$

ψ_A : Vehicle orientation angle between global coordinate X axis and vehicle local coordinate x-axis measured in counter-clockwise direction (rad)

β_A : Vehicle sideslip angle between vehicle local coordinate x-axis and the vehicle velocity direction measured in counter-clockwise direction (rad)

ψ_R : Reference orientation angle (rad)

β_R : Reference sideslip angle (rad)

l_{fr}, l_{re} : Longitudinal distances from vehicle center of gravity (CG) to the front and rear wheels, respectively (m)

b : Lateral distances from CG to right or left wheel (m)

X_R, Y_R : Reference positions of the object

The kinematic equation for this 4WIS-AGV configuration obtained by 'single track vehicle model' i.e., reducing an ordinary four wheel vehicle model into a two wheel vehicle model with the wheels at the centerline of the vehicle is expressed as follows [9]:

$$\begin{bmatrix} \dot{X}_A \\ \dot{Y}_A \\ \dot{\psi}_A \\ \dot{\beta}_A \end{bmatrix} = \begin{bmatrix} \cos(\psi_A + \beta_A) & 0 & 0 \\ \sin(\psi_A + \beta_A) & 0 & 0 \\ 0 & 1 & 0 \\ 0 & 0 & 1 \end{bmatrix} \begin{bmatrix} v_A \\ \dot{\psi}_A \\ \dot{\beta}_A \end{bmatrix}. \tag{1}$$

The vehicle angular velocity $\dot{\psi}_A$ and the i^{th} wheel velocities v_i of the 4WIS-AGV can be calculated as follows:

$$\dot{\psi}_A = \frac{v_A \cos\beta_A \left(\tan\delta_{fr} - \tan\delta_{re}\right)}{l_{fr} + l_{re}}, \tag{2}$$

$$v_i = \begin{cases} \dfrac{v_A \tan\delta_{fr} \csc\delta_i}{\sqrt{1 + \frac{1}{4}\left(\tan\delta_{fr} + \tan\delta_{re}\right)^2}}, \\ i = 1,2; \cos\delta_{fr} \sin\delta_i \neq 0, \delta_i \neq \delta_{fr}, \\ \dfrac{v_A \tan\delta_{re} \csc\delta_i}{\sqrt{1 + \frac{1}{4}\left(\tan\delta_{fr} + \tan\delta_{re}\right)^2}}, \\ i = 3,4; \cos\delta_{re} \sin\delta_i \neq 0, \delta_i \neq \delta_{re} \end{cases} \tag{3}$$

In this paper, zero-sideslip maneuver is considered for the 4WIS-AGV [9]. Therefore, the sideslip angle β_A is kept zero while the vehicle moves. For the zero-sideslip maneuver, steering angles of the front and rear wheels: δ_{fr} and δ_{re} of the 4WIS-AGV can be obtained as follows:

$$\delta_{re} = \tan^{-1}\left(\frac{-l_{re}\tan\delta_{fr}}{l_{fr}}\right), \tag{4}$$

$$\delta_{fr} = \tan^{-1}\left(\frac{\dot{\psi}_A l_{fr}}{v_A}\right). \tag{5}$$

Subsequently, the steering angles of each wheel, δ_i, can be calculated as follows:

$$\begin{cases} \delta_{1,2} = \cot^{-1}\left(\cot\delta_{fr} \pm \dfrac{b}{l_{fr}+l_{re}}\cot\delta_{fr}\left[\tan\delta_{fr} - \tan\delta_{re}\right]\right), \\ for\ \ \delta_{1,2} \neq \delta_{fr}, \delta_{fr} \neq \delta_{re}, \cos\delta_{re}\sin\delta_{fr} \neq 0 \\ \delta_{3,4} = \cot^{-1}\left(\cot\delta_{re} \mp \dfrac{b}{l_{fr}+l_{re}}\cot\delta_{re}\left[\tan\delta_{fr} - \tan\delta_{re}\right]\right), \\ for\ \ \delta_{3,4} \neq \delta_{re}, \delta_{fr} \neq \delta_{re}, \cos\delta_{fr}\sin\delta_{re} \neq 0. \end{cases} \tag{6}$$

4. OBJECT POSITION MEASUREMENT

In this section, firstly, the center coordinates of the candidate blue colored object in pixel are obtained. Secondly, using trigonometric laws and depth data from the Kinect camera, these pixel coordinates are converted into the real coordinates in meter. Thirdly, the real coordinates are transformed to the global coordinate frame. Finally, based on the object motion model, the Kalman filter algorithm is used to estimate the global position coordinates of the moving candidate object.

A color-based object detection algorithm based on Aforge.NET C# framework is used to obtain the candidate blue colored object position coordinates inside the Kinect RGB image frames [10]. Fig. 3 shows an extended vertical field of view from the Kinect camera sensor (43^o) showing the real candidate object and the detected candidate object inside the RGB image.

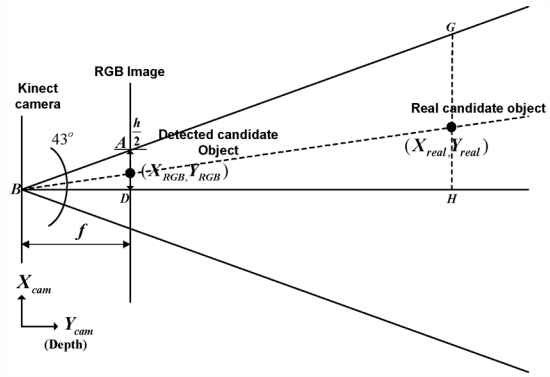

Fig. 3 Extended vertical view from the Kinect camera sensor.

where

(X_{RGB}, Y_{RGB}): Candidate object center coordinates inside RGB image (pixels)

(X_{real}, Y_{real}): Candidate object real coordinates (m)

By applying simple trigonometry, it can be written as,

$$f = \frac{h}{2\tan(43/2)}, \tag{7}$$

where

f: Constant of conversion (pixels)

$h = 480$: Height of the RGB image screen (as the RGB image screen resolution is 640×480) (pixels)

Using the property of similar triangles, it can be written as,

$$\frac{X_{RGB}}{f} = \frac{X_{real}}{Y_{real}}, \tag{8}$$

where Y_{real} represents the depth in meter obtained directly from the Kinect depth data.

Therefore, by calculating f using Eq. (7), the pixel position coordinate X_{RGB} is converted to real position coordinate X_{real} in meter as follows:

$$X_{real} = \frac{X_{RGB} Y_{real}}{f}. \tag{9}$$

In Fig. 2, the real position (X_{real}, Y_{real}) of the object can be transformed to global position (X_o, Y_o) as follows:

$$\begin{bmatrix} X_o \\ Y_o \end{bmatrix} = \begin{bmatrix} X_A \\ Y_A \end{bmatrix} + \begin{bmatrix} \cos(\psi_A - 90^o) & -\sin(\psi_A - 90^o) \\ \sin(\psi_A - 90^o) & \cos(\psi_A - 90^o) \end{bmatrix} \begin{bmatrix} X_{real} \\ Y_{real} \end{bmatrix} + \begin{bmatrix} \cos\psi_A \\ \sin\psi_A \end{bmatrix} D. \tag{10}$$

where $D = 0.45$ m is the distance between the Kinect camera sensor and the NAV200 placed on 4WIS-AGV.

Since the Kinect camera sensor has some noise and sometimes it detects unwanted objects due to different real-time conditions, it is difficult to keep the track the position coordinates of the candidate moving object. To deal with this problem, the Kalman filter is used in this paper as follows.

The position and velocity coordinates of the object with respect to OXY coordinate frame can be written as the following state space

$$\mathbf{x}_k = \begin{bmatrix} X_o & Y_o & \dot{X}_o & \dot{Y}_o \end{bmatrix}^T. \tag{11}$$

The discrete time dynamic behavior of the object is represented by the state vector $\mathbf{x}_k$ at time *k* as follows:

$$\mathbf{x}_k = \mathbf{F}\mathbf{x}_{k-1} + \mathbf{w}_k, \tag{12}$$

where $\mathbf{F} = \begin{bmatrix} 1 & 0 & T & 0 \\ 0 & 1 & 0 & T \\ 0 & 0 & 1 & 0 \\ 0 & 0 & 0 & 1 \end{bmatrix}$ is the transition matrix, $\mathbf{w}_k$ is the Gaussian process noise with covariance matrix $\mathbf{Q}$ at time *k* and *T* is the sampling time.

The measurement $\mathbf{z}_k$ of the true position of an object obtained from the Kinect camera sensor at time *k* is expressed as follows:

$$\mathbf{z}_k = \mathbf{H}\mathbf{x}_k + \mathbf{v}_k, \tag{13}$$

where $\mathbf{H}=\begin{bmatrix}1&0&0&0\\0&1&0&0\\0&0&1&0\\0&0&0&1\end{bmatrix}$ is the measurement matrix and $\mathbf{v}_k$ is the Gaussian measurement noise with covariance matrix $\mathbf{R}$ at time k.

The Kalman filter exhibit two steps: prediction and update step as follows:

- Prediction step:

$$\begin{cases}\hat{\mathbf{x}}_k^- = \mathbf{F}\hat{\mathbf{x}}_{k-1},\\ \mathbf{P}_k^- = \mathbf{F}\mathbf{P}_{k-1}\mathbf{F}^T + \mathbf{Q},\end{cases} \tag{14}$$

where $\hat{\mathbf{x}}_k^-$ is the predicted state estimation at time k and $\mathbf{P}_k^-$ is the predicted covariance matrix estimation a t time k.

- Update step:

$$\begin{cases}\mathbf{K}_k = \mathbf{P}_k^-\mathbf{H}^T(\mathbf{H}\mathbf{P}_k^-\mathbf{H}^T + \mathbf{R})^{-1},\\ \hat{\mathbf{x}}_k = \hat{\mathbf{x}}_k^- + \mathbf{K}_k(\mathbf{z}_k - \mathbf{H}\hat{\mathbf{x}}_k^-),\\ \mathbf{P}_k = (\mathbf{I} - \mathbf{K}_k\mathbf{H})\mathbf{P}_k^-.\end{cases} \tag{15}$$

where $\mathbf{K}_k$ is the Kalman gain at time k, $\hat{\mathbf{x}}_k$ is the updated state estimation at time k and $\mathbf{P}_k$ is the updated covariance matrix estimation at time k.

5. CONTROLLER DESIGN

The control objective is to track the reference position (X_R, Y_R) with keeping a given safe distance between 4WIS-AGV and a moving object. The safe distance is chosen as $D_{ref} = 1.25$ m.

The reference position coordinates (X_R, Y_R) can be obtained as follows:

$$\begin{bmatrix}X_R\\Y_R\end{bmatrix} = \begin{bmatrix}\hat{X}_o\\\hat{Y}_o\end{bmatrix} - \begin{bmatrix}\cos\psi_A\\\sin\psi_A\end{bmatrix} D_{ref}, \tag{16}$$

where $\hat{X}_o, \hat{Y}_o$ are the estimated positions of the moving object by Kalman filter.

For the 4WIS-AGV to follow the moving object well, the linear velocity of 4WIS-AGV should be same as the moving object velocity. Therefore, the reference linear velocity v_R is expressed as follows:

$$v_R = \dot{\hat{X}}_o \cos\psi_R + \dot{\hat{Y}}_o \sin\psi_R, \tag{17}$$

where $\dot{\hat{X}}_o, \dot{\hat{Y}}_o$ are the estimated velocities of the object by using Kalman filter.

The reference orientation angle ψ_R is calculated as follows:

$$\psi_R = \arctan\left(\frac{\hat{Y}_o - Y_A}{\hat{X}_o - X_A}\right). \tag{18}$$

In Fig. 2, a tracking error vector $\mathbf{e}$ can be defined as follows:

$$\mathbf{e} = \begin{bmatrix}e_1\\e_2\\e_3\\e_4\end{bmatrix} = \begin{bmatrix}\cos\psi_A & \sin\psi_A & 0 & 0\\ -\sin\psi_A & \cos\psi_A & 0 & 0\\ 0 & 0 & 1 & 0\\ 0 & 0 & 0 & 1\end{bmatrix}\begin{bmatrix}X_A - X_R\\Y_A - Y_R\\\psi_A - \psi_R\\\beta_A - \beta_R\end{bmatrix}, \tag{19}$$

where

e_1: Error in local coordinate x-axis (m)

e_2: Error in local coordinate y-axis (m)

e_3: Vehicle orientation error with respect to the reference orientation (rad)

e_4: Vehicle sideslip angle error with respect to the reference sideslip angle (rad).

To minimize these errors i.e., to make the 4WIS-AGV to follow the moving object, a controller based on backstepping control method is designed for the 4WIS-AGV.

Using the backstepping control method, a candidate Lyapunov function (clf) is chosen as follows :

$$V = \frac{1}{2}e_1^2 + \frac{1}{2}e_2^2 + \frac{1}{k_2}(1-\cos e_3) + \frac{1}{2}e_4^2, \text{ for } k_2 > 0, \tag{20}$$

The time derivative of clf $\dot{V}$ is obtained as follows:

$$\dot{V} = e_1\dot{e}_1 + e_2\dot{e}_2 + \frac{1}{k_2}\sin e_3\dot{e}_3 + e_4\dot{e}_4. \tag{21}$$

Because the 4WIS-AGV cannot move sideways without adjusting its wheels to the side direction under no slip and pure rolling, a nonholonomic constraint can be applied as expressed in Eq. (22) as follows:

$$\begin{cases}\dot{X}_R\sin\psi_R - \dot{Y}_R\cos\psi_R = 0,\\ \dot{X}_A\sin\psi_A - \dot{Y}_A\cos\psi_A = 0.\end{cases} \tag{22}$$

From Eq. (19) and Eq. (22), the time derivative of tracking error vector $\dot{\mathbf{e}}$ is written as follows:

$$\dot{\mathbf{e}} = \begin{bmatrix}-v_R\cos e_3\\ v_R\sin e_3\\ -\dot{\psi}_R\\ -\dot{\beta}_R\end{bmatrix} + \begin{bmatrix}1 & e_2 & 0\\ 0 & -e_1 & 0\\ 0 & 1 & 0\\ 0 & 0 & 1\end{bmatrix}\begin{bmatrix}v_A\\\dot{\psi}_A\\\dot{\beta}_A\end{bmatrix}. \tag{23}$$

Substituting (23) in (21) yields

$$\dot{V} = e_1(v_A - v_R\cos e_3) + \frac{1}{k_2}\sin e_3(\dot{\psi}_A - \dot{\psi}_R + e_2k_2v_R) + e_4(\dot{\beta}_A - \dot{\beta}_R). \tag{24}$$

According to the Lyapunov stability criterion, if $\dot{V} \le 0$, the system is stable. Therefore, to achieve this condition, a control law U can be chosen as follows:

$$U = \begin{bmatrix}v_A\\\dot{\psi}_A\\\dot{\beta}_A\end{bmatrix} = \begin{bmatrix}-k_1e_1 + v_R\cos e_3\\ \dot{\psi}_R - e_2k_2v_R - k_3\sin e_3\\ \dot{\beta}_R - k_4e_4\end{bmatrix}, \tag{25}$$

where k_1, k_2, k_3 and k_4 are positive constants.

Substituting Eq. (24) in Eq. (23), the derivative of clf can be expressed as follows:

$$\dot{V} = -k_1e_1^2 - \frac{k_3}{k_2}\sin^2 e_3 - k_4e_4^2. \tag{26}$$

which shows that the value of $\dot{V} \le 0$ by using the chosen control law. In other words, the system becomes stable when $e_1, e_3, e_4 \to 0$ as $t \to \infty$ using Eq. (22),

Eq. (24), Eq. (25) and Barbalet's lemma. In case of $e_1, e_2, e_4 \to 0$ as $t \to \infty$ and $\dot{\psi}_A \neq 0$, from Eq. (23) and Eq. (25), $e_2 \to 0$ can be obtained.

Fig. 4 shows the block diagram of the proposed object tracking and following system using 4WIS-AGV with Kinect camera sensor.

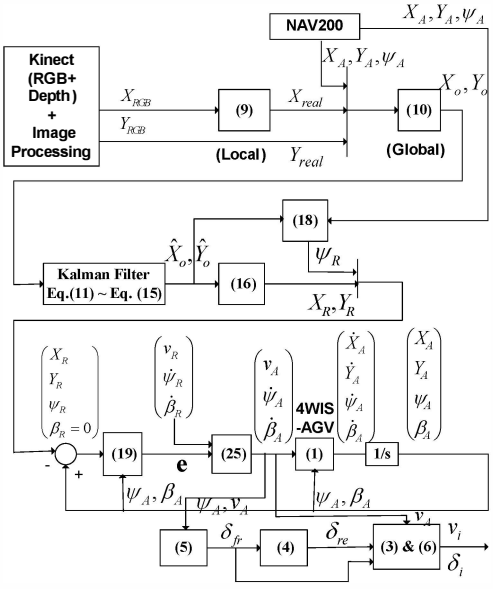

Fig. 4 Block diagram of the proposed system.

6. SIMULATION AND EXPERIMENTAL RESULTS

Simulation and experiment are done to verify the effectiveness of the designed controller. The parameters and their initial values for simulation are shown in Table I.

Table 1 Parameters and initial values for simulation.

Descriptions	Symbols	Values
Initial position of the 4WIS-AGV	$(X_A(0), Y_A(0))$	(0, 0) m
Initial position of the candidate object	$(X_o(0), Y_o(0))$	(3, -2) m
Value of object velocity in X direction	$\dot{X}_o$ *for* $(t = 0-30\text{s})$	0.1 m/s
Value of object velocity in Y direction	$\dot{Y}_o$ *for* $(t = 0-30\text{s})$	-0.1 m/s
Controller gain 1	k_1	1 s^{-1}
Controller gain 2	k_2	1 rad/m^2
Controller gain 3	k_3	0.5 rad/s
Controller gain 4	k_4	1 s^{-1}

The comparison of simulation and experimental results are shown in Fig. 5 and Fig. 6. For the sake of simplicity, in both the cases, the object stops at 30 sec. The values of object velocity coordinates is as shown in Table 1. Fig. 5 shows the results for tracking errors. In the simulation case, the errors $e_1, e_2, e_3, e_4 \to 0$ at 10 s, 5 s, 3 s, 0 s respectively. In the experimental case, the errors $e_1, e_2, e_3, e_4 \to 0$ at 25 s, 30 s, 35 s, 0 s respectively. The results for the control law U are shown in Fig. 6. This figure shows the linear velocity, angular velocity and the sideslip angular velocity of the 4WIS-AGV. In both results, the vehicle linear velocity gradually decreases to about 0.15 m/s and then renains constant until 30 s and then converges to zero. In the simulation result, the angular velocity converges to zero after 3 s, whereas in the experimental result, it converges to zero after 10 s. In this paper, since the sideslip angle β_A is kept zero, therefore the vehicle sideslip angular velocity $\dot{\beta}_A = 0$.

In the simulation, only kinematic problem of the 4WIS-AGV is considered. However, in the experiment, real time conditions such as effect of ground friction, sensor noise, etc., can't be ignored. Moreover, the object velocity is not constant since the object is moved manually. Therefore, simulation and experimental results have some differences between them.

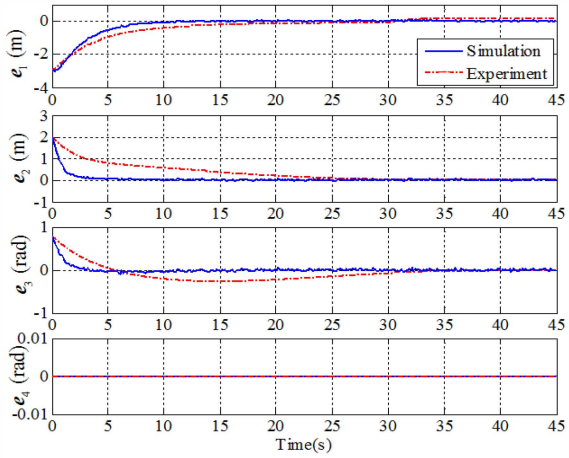

Fig. 5 Tracking errors.

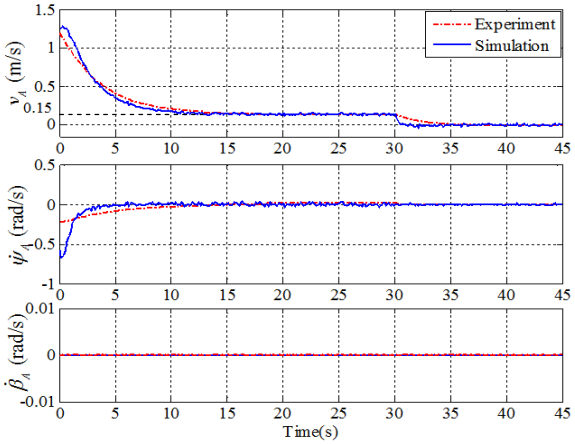

Fig. 6 Control law U.

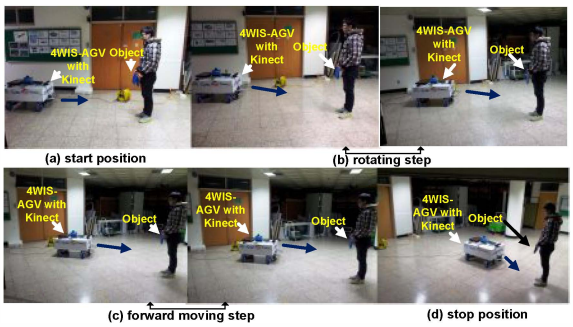

Fig. 7 Images showing sequence of events occurred during object following of the 4WIS-AGV system.

The experiment is performed to verify the performance of the proposed system and its results are shown in Fig. 7. For the sake of simplicity, the sequence of events occurred during the object following of the 4WIS-AGV system is explained as follows: Fig. 7(a) shows the start position of the 4WIS-AGV with Kinect camera sensor. In this case, the candidate blue colored object is placed at a distance more than 1.2 m from the 4WIS-AGV system. Fig. 7(b) shows the rotating step of the 4WIS-AGV system. In this case, after the successful detection of the blue colored object, the 4WIS-AGV system tracks the position of the detected object and changes its orientation towards it. Fig. 7(c) shows the forward moving step of the 4WIS-AGV system. In this event, the object moves forward and the 4WIS-AGV tracks and follows the moving object. Fig. 7(d) shows the stop position of the 4WIS-AGV. In this case, the moving object stops as shown in Fig. 7(d). The 4WIS-AGV continues to follow the stop object until the distance between the object and the 4WIS-AGV becomes equal to the reference distance (1.25 m). When the distance between the 4WIS-AGV and the moving object is equal to the reference distance, the 4WIS-AGV stops following the object.

7. CONCLUSION

This paper proposed the moving object tracking and following control of the 4WIS-AGV system using Kinect camera sensor. The following steps were executed to achieve object tracking and following. The 4WIS-AGV system was developed with the Kinect camera sensor and the NAV 200 positioning sensor and its kinematic modeling was presented. Image processing was done using Kinect camera sensor to detect the position of the candidate object inside the RGB image frames. Using Kinect depth data and NAV 200 sensor data, global position coordinates of the candidate object were obtained. The position and velocity coordinates of the moving candidate object were tracked using the Kalman filter. Based on the kinematic modeling, the backstepping control method using Lyapunov function was designed for the 4WIS-AGV to achieve object following task. Finally, the simulation and experimental results verified the effectiveness of the proposed system. The results showed that with the proposed control algorithm, the Kinect-based 4WIS-AGV system can follow the moving object successfully.

ACKNOWLEDGMENT

This study is a part of the results of the R&D project supported by the preparatory association of Pukyong National University. Authors are debt to appreciate Pukyong National University for their full supports to this pioneering work.

REFERENCES

[1] L. Dong and X. Lin, "Monocular-vision-based study on moving object detection and tracking," *Proc. of the 4th International Conference on New Trends in Information Science and Service Science (NISS)*, pp. 692–695, 2010.

[2] P. K. Das, S. C. Mandhata, C. N. Panda and S. N. Patro, "Vision based object tracking by mobile robot," *International Journal of Computer Applications*, Vol. 45, No. 8, pp. 40–42, 2012.

[3] G. Xing, S. Tian, H. Sun, W. Liu and H. Liu, "People-following system design for mobile robots using Kinect sensor," *Proc. of the 25th Chinese Control and Decision Conference (CCDC)*, pp. 3190–3194, 2013.

[4] N. Mir-Nasiri, "Camera-based 3D object tracking and following mobile robot," *Proc. of the 2006 IEEE Conference on Robotics, Automation and Mechatronics*, pp. 1–6, 2006.

[5] B. F. Buxton, D. A. Castelow, M. Rygol, P.F. Mclauchlan and S. B. Pollard, "Developing a stereo vision system for control of an AGV," *Proc. of the 2nd International Specialist Seminar on the Design and Application of Parallel Digital Processors*, pp. 79–83, 1991.

[6] I. Ullah, F. Ullah and Q. Ullah, "Real-time object following fuzzy controller for a mobile robot", *Proc. of the 2011 International Conference on Computer, Networks and Information Technology*, pp. 241-244, 2011.

[7] K. Kinoshita and K. Murakami, "Moving object tracking via one-dimensional optical flow using queue," *Proc. of the 10th International Conference on Control, Automation, Robotics and Vision,* pp. 2326-2331, 2008.

[8] A. Ahmad and P. Lima, "Multi-Robot Cooperative Spherical-Object Tracking in 3D Space Based on Particle Filters", *Proc. of the 5th European Conference on Mobile Robotics*, pp. 1084-1093, 2013.

[9] D. Wang and F. Qi, "Trajectory planning for a four-wheel-steering-vehicle," *Proc. of the IEEE International Conference on Robotics and Automation*, pp. 3320-3325, 2011.

[10] A. V. Gulalkari, G. Hoang, P. S. Pratama, H. K .Kim, S. B. Kim and B. H. Jun, "Object following control of six-legged robot using Kinect camera," *Proc. of the 3rd International Conference on Advances in Computing, Communications and Informatics*, pp. 758-764, 2014.